Mechanical, Thermal, and Barrier Properties of NBR/Organosilicate Nanocomposites

WEI-GWO HWANG *and* KUNG-HWA WEI*

Department of Materials Science and Engineering
National Chiao Tung University
Hsinchu, Taiwan 30049, R.O.C.

CHANG-MOU WU

Applied Science & Technology Research Center
Department of Environmental Resources Management
Transworld Institute of Technology
Yunlin, Taiwan 64063, R.O.C.

Nanocomposites of intercalated and exfoliated organosilicates in acrylonitrile butadiene rubber (NBR) were prepared by a solution-blending method. The dispersion and intergallery spacings of organosilicates in these nanocomposites were examined by transmission electron microscopy and X-ray diffraction. Dramatic enhancements in the mechanical and thermal properties of NBR are found by incorporating less than ten parts of organosilicate. In particular, the addition of ten parts of organosilicate provided a more than sixfold increase in tensile strength, a twofold increase in M500, and 168% and 39% enhancements in tear strength and elongation at break compared with pure NBR. The degradation temperature for NBR with ten-parts' loading of organosilicate was 25°C higher than that of pure NBR. In addition, the relative vapor permeability of the NBR nanocomposites for water and methanol were 85% and 42% lower, respectively, than that of pure NBR. Polym. Eng. Sci. 44:2117–2124, 2004.

INTRODUCTION

The pioneering work conducted by Toyota Central Research on nylon-6/silicate nanocomposites has inspired great interest in polymer nanocomposites over the past decade (1–3). This particular interest results from the highly efficient enhancement of the barrier and mechanical properties of a polymer by the nanometer-sized silicates when they are well dispersed in the polymer matrix. The ideal case would have the layered silicates completely separated from one another (termed delaminated or exfoliated) in the polymer matrix. In the other case, there would be a slight increase in the intergallery spacing of the layered silicates but the same orientation for most of layered silicates (termed intercalated) is retained in the matrix. Exfoliation, however, can hardly be achieved in silicates without modification by small organic molecules, which diffuse readily into the intergallery of the silicate layers and open up with enough space between silicates to allow further penetration of the polymer molecules. The driving force for exfoliation or intercalation depends upon the thermodynamic interaction between polymer and silicate as well as the diffusion of polymer chains into the intergallery of the silicate layers. In most cases, proper chemical treatment and optimized processing are key to the formation of nanocomposites. The interlayer distance of the montmorillonite-based silicates when modified with alkylammonium cations is between 1.5 and 3.5 nm. This space is usually large enough to produce intercalated and exfoliated structures upon further processing. *In-situ* polymerization, polymer intercalation from solution, and direct polymer melt intercalation have been developed to prepare polymer-layered silicate nanocomposites (4, 5).

While organosilicates have been used in various thermoplastics and thermoset resins, a fairly small number

*To whom correspondence should be addressed. E-mail: khwei@cc.nctu.edu.tw

Published online in Wiley InterScience (www.interscience.wiley.com).
DOI: 10.1002/pen.20217

of studies have been reported on the use of organosilicates to reinforce rubber. "Bound rubber," a traditional concept, can be used to demonstrate the reinforcing behavior of rubber with carbon black or layered silicates, which is an undissolved composition of rubber compound by solvent (6–8). Bound rubber based on carbon black would cause a considerable increase in compounding viscosity and is disadvantageous in the mixing process. Another drawback of carbon black is that it has a black color and is usually used in high amounts, which is detrimental to the final performance of rubber formulations. A variety of white or pale fillers have been chosen to replace carbon black, such as silica or clay minerals. The reinforcing effect of NBR nanocomposites containing a few weight-percent of layered silicates is similar to NBR compounds having a much higher loading of carbon black. When using properly treated organosilicate, however, it can provide an effective physical reinforcement, helping to reduce the viscosity of the uncured elastomeric compound and also retain transparency (8–10).

Additionally, the efficiency of the silicates in modifying the properties of the rubber is largely determined by the degree of their dispersion and the extent of exfoliation in the rubber. Rubbers are more hydrophobic than some thermoplastics, such as nylon 6, and therefore, it is difficult to achieve dispersion of layered silicates in a rubber matrix by treating montmorillonite with alkyl ammonium ions alone. There are, however, some advantages for rubber/silicate nanocomposites. First, amine-compounds are widely used in sulfur curing rubber formulations as accelerators, and hence the ammonium molecule in the montmorillonite might be involved in the sulfur curing reaction. Besides, the very high molecular weight rubber material implies that high shear stress will be generated locally during compounding, which is beneficial to the delamination of layered silicates. Hence, compounding with the proper rubber formulation design allows the intercalation and delamination of silicate layers in rubber to become possible (11). From the literature, the use of organosilicates as precursors for the nanocomposite formations has been extended into various elastomer systems including natural rubber (NR) (12–14), epoxidized natural rubber (ENR) (6, 15), styrene butadiene rubber (SBR) (9, 16), ethylene-propylene-diene rubber (EPDM) (2, 17), nitrile butadiene rubber (NBR) (18–20), polyurethane elastomer (10, 21–23), and silicone rubber (24, 25). The compounding methods used in these cases can be categorized as solution blending, melt mixing and latex compounding. It has been shown that solution blending is a reproducible method to intercalate the rubber molecules into the silicate galleries. Solution blending of polar NBR rubber and layered silicates has not yet been reported.

In order to study in more detail the reinforcing effect of organosilicate in rubbers, NBR was selected to produce nanocomposites by solution blending with hydrophobic organosilicates. NBR has high polarity and is one of the most important industrial raw materials. The effect of the amount of organosilicate on the mechanical, thermal and barrier properties of these nanocomposites was investigated in the present study. In addition, the thermodynamical behavior of NBR/layered silicate nanocomposites was also studied.

EXPERIMENTAL

Material Preparation

Acrylonitrile-butadiene rubber (NBR, Nipol N32, acrylonitrile content 32%, Zeon Inc., Japan) was selected as the rubber matrix. Organosilicate intercalated by dimethyl, dehydrogenated tallow, and quaternary ammonium (Cloisite 15A, Southern Clay Products Inc.) with aspect ratio 75–100 were used in this work. For comparison, conventional carbon black (CB, N-220, China Synthetic Rubber, Taiwan) and silica (Aerosil, Degussa, Germany) were also mixed with NBR in a two-roll mixing mill directly. The composition used in this study is given in *Table 1*.

The mixing of the organosilicate with elastomer was facilitated by the use of solvent (6, 26). NBR was dissolved in methyl ethyl ketone (MEK). The organosilicates were also swollen in MEK independently and then mixed with the NBR solution with vigorous stirring for 12 hr. The MEK in the resulting dispersion was then evaporated and the sample dried under vacuum for 2 days. After that, the resulting organosilicate-reinforced NBR was mixed with the additives and sulfur in a two-roll mill. The samples were then cured at 160°C in an electrically heated hydraulic press to their respective cure times, t_{90}. These values were derived from a Monsanto oscillating disc rheometer (MDR 2000), cf. *Table 2*.

Table 1. Formulation of NBR Compounds.

Material	phr
NBR	100
Organosilicate	0-10 (various)
ZnO	5
Stearic acid	2
Sulfur	1.5
Accelerators	2.2

phr: parts per hundred rubber.

Table 2. Vulcanization Characteristics of NBR Compounds.

Organosilicate Content (phr)	t_2 (sec)	t_{90} (sec)	M_L (lb-in)	M_H (lb-in)	M_H-M_L (Nm)
0	106	382	0.40	5.48	5.06
1	88	383	0.40	5.60	5.20
3	87	409	0.41	5.62	5.21
5	89	412	0.45	6.26	5.81
7.5	91	412	0.57	6.44	5.87
10	87	412	0.67	6.85	6.18

t_2 : initial scorch time to 2 units of torque increase above minimum torque.
t_{90} : cure time to 90% of maximum torque development.
M_L : minimum torque.
M_H : maximum equilibrium torque.
M_H-M_L : torque increase.

Characterization

Tensile and tear tests were performed on dumbbell-shaped specimens, following ASTM standards D 412 and D 624, respectively, on a material-testing system machine (Sintech, MTS) at a crosshead speed of 50 cm/min. For each data point, five specimens were tested, and the average value was taken. Hardness was directly measured by a hardness meter (Teclock, Japan) according to ASTM D 2240 standards. Fourier-transform infrared spectroscopy (FTIR) experiments were performed with a PerkinElmer IR2000 spectrometer over a frequency range of 650−4000 cm^{-1}. The samples for the FTIR study were prepared with cured NBR compounds using compression molding. Thermogravimetric analysis (TGA) of each sample was carried out under nitrogen purge in a PerkinElmer TGA-7. About 10 mg of cured sample was heated from 50°C to 750°C at 10°C/min. Dynamic-mechanical thermal analysis (DMA7, PerkinElmer) spectra were recorded on rectangular specimens (length × width × thickness = 6 × 1 × 0.25 cm^3) in tensile mode at a frequency of 10 Hz. DMTA spectra, viz. storage modulus and mechanical loss factor (tanδ), were measured in the temperature range from −100°C to 70°C at a heating rate of 5°C/min.

The XRD patterns of the rubber samples were obtained on a D5000 diffractometer (Siemens, Munich, Germany) using Ni-filtered CuK_α radiation (λ = 0.1542 nm). The samples were scanned in step mode at a 1.5°/min scan rate in the range of $2\theta < 10°$. The TEM was a JEOL JEM 2000FX electron microscope operating with an acceleration voltage of 200 kV. Ultrathin sections of the cured samples were microtomed using Leica Ultracut, cut with a diamond knife into slices approximately about 100 nm thick; subsequently, a layer of carbon was deposited onto these slices and placed on 400-mesh copper nets. The crosslinking density was determined by equilibrium swelling. Swelling experiments were carried out with cured samples by putting the samples in toluene at 25°C for 48 hr in order to achieve the equilibrium swelling condition. The uptake solvent percentage, Q, and volume fraction of NBR in the swollen gel, Vr, were calculated with the following equations:

$$Q = (M_{sw} - M_i)/M_i \tag{1}$$

where M_i and M_{sw} are the weight of the rubber sample before immersion in the solvent and the swollen state, respectively.

$$Vr = (1/D_{sam})/[(1/D_{sam}) + (Q/D_{sol})] \tag{2}$$

where D_{sam} and D_{sol} are the densities of the rubber sample and solvent (0.87 for toluene).

The crosslinking density of the sample, ν, defined by the number of elastically active chains per unit volume, was calculated by the Flory-Rehner equation (27):

$$\nu = -\frac{\ln(1 - Vr) + Vr + \chi\, Vr^2}{Vs\,(Vr^{1/3} - Vr/2)} \tag{3}$$

where Vs is the molar volume of the swelling solvent (106.1 cm^3/mol for toluene). χ is the Flory-Huggins (rubber-toluene) interaction parameter and was taken as 0.435 for the NBR-toluene system in this calculation.

Thermodynamical aspects of rubber elasticity are crucial to obtain a deeper understanding of mixing in NBR/silicate nanocomposites. The expansion of rubber in the presence of a solvent will significantly modify the conformational entropy (ΔS) and the elastic Gibbs free energy (ΔG). The elastic Gibbs free energy can be determined from the Flory-Huggins equation (11, 14):

$$\Delta G = RT\,[\ln(1 - Vr) + Vr + \chi\, Vr^2] \tag{4}$$

From the statistical theory of rubber elasticity, the conformational entropy ΔS can be obtained from $\Delta G = -T\Delta S$, which assumes that no changes in the internal energy of the network occurs upon stretching.

The water and solvent (methanol) vapor transmission were measured at 40°C and 50% relative humidity, according to ASTM E96. To minimize the influence of thickness on the vapor transmission, the thickness of the sample is set to be 5 mm by molding. The permeability, P, is calculated by the following equation:

$$P = 6237 \times (W - W_1) \tag{5}$$

where W and W_1 are the weights of the sample assembly before and after testing, respectively. The relative permeability was defined as the measured permeability divided by the pure NBR permeability.

RESULTS AND DISCUSSION

The curing characteristics are summarized in *Table 2*. In the presence of organosilicates, the initial scorch time, t_2 (about 89 sec), was shorter than that of pure NBR (106 sec). This is because the acidic nature of organosilicate activates the formation of soluble zinc ions. The soluble zinc ions in turn induce the decomposition of accelerator into free radicals in the earlier reaction stage. These free radicals cause the premature vulcanization and result in a decrease of the scorch time. The cure time of NBR nanocomposites, t_{90}, increased with the content of the organosilicate. This result is different from the catalytic effect reported in some of the NR/organosilicate nanocomposite literature (15). It can be attributed to the greater acidity of the organosilicates, which exhausts some decomposed accelerator free radicals in the following crosslinking reaction, retarding curing and influences the kinetics of the crosslinking reaction. Another possible cause (28) is the ZnO, which neutralizes the most active sites of the filler surface and has been proven in silica. Both M_L and M_H of these nanocomposites increase with the amount of organosilicate, effectively resulting in an increase in the stiffness of the NBR matrix. The increasing stiffness, $M_H - M_L$, corresponds with the increasing hardness tested results as given in *Table 2*.

Dispersion of the Silicates

The efficiency of organosilicate in reinforcing the polymer matrix is primarily determined by the degree of

its dispersion in the matrix and the extent of intercalation of organosilicate by polymer molecules. *Figure 1* shows the (001) diffraction peak of the organosilicate is shifted to lower diffraction angles in the nanocomposite as compared to that of the pure organosilicate. The d-spacings of the stacks were 3.53−4.26 nm for the NBR/organosilicate nanocomposites, whereas it is 3.15 nm for the pure organosilicate. In the NBR nanocomposites containing 3 parts of layered silicates has the largest interlayer distance, 4.26 nm. At low silicate loading, the viscosity of the nanocomposite is not large enough to generate a sufficient shearing force for moving the majority of rubber molecules to intercalate into the layered silicates gallery. Hence, the increase in the d-spacing of layered silicate is limited. At high silicate loading, the dispersion of layered silicates is difficult, but a high shear force has been resulted for moving large rubber molecules to intercalate into the layered silicates gallery. Therefore, a compromise was reached by the two factors at about 3 parts' silicate loading. This indicates that an optimum loading of organosilicate in the NBR case has been obtained. The peaks around 4.18°−4.93° and 6.0°−7.0° result from higher order diffractions from the (002) and (003) diffraction planes, respectively. The multi-diffraction peaks reflect a well-defined layered silicate structure. In the case of 1-phr organosilicate in NBR, a lower but strong peak around 6.50° (1.36 nm) was displayed. It has been attributed to the thermal degradation and desoption of the organic materials in the gallery (29). In this study, however, the NBR nanocomposites were prepared by solution blending without a high-temperature mixing process. Thus, it is speculated to be an effect of the organosilicate confinement (reaggregation) (10, 15). The formation of a zinc-sulfur accelerator complex "extracts" the amine intercalant of the organosilicates, thus causing the collapse of the layers. *Figure 2* shows the TEM image of the NBR nanocomposite containing 7.5-phr organosilicate. Most of the layered silicates are well distributed in the NBR matrix, and a large portion of the organic-modified silicate layer particles appear to be interlated along with a few single delaminated platelets. No visible differences in the morphology of any of the NBR/organosilicate samples can be found. The TEM result is in consistent with that of the XRD study, as shown in *Fig. 1*. Both TEM and XRD results thus confirm that the layers of the organosilicate particles have been intercalated successfully in the NBR nanocomposites.

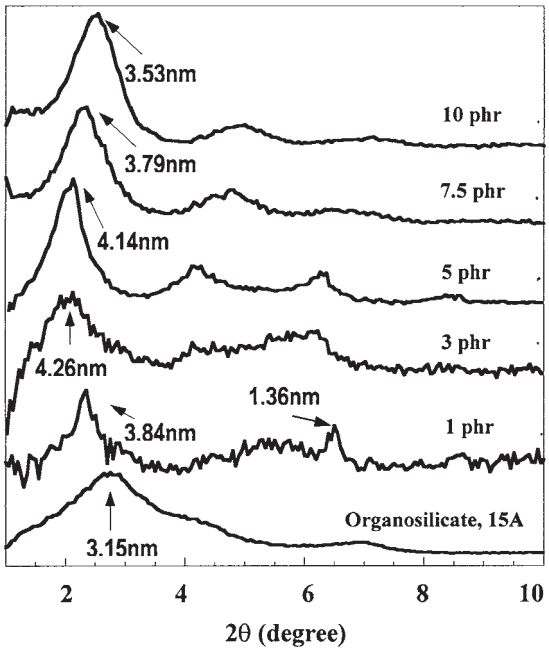

Fig. 1. X-ray diffraction patterns of NBR nanocomposites with various organosilicate contents.

Mechanical Properties

Figure 3 shows stress-strain curves in tensile for the NBR nanocomposites containing different amounts of organosilicate. The tensile properties of these nanocomposites increase with the amount of organosilicate. At high strains, stress-hardening behavior is observed for the NBR incorporating organosilicate. *Table 3* summarizes the ultimate properties of tensile strength, elongation at break, modulus at 100%, 300% and 500% elongation, and tear strength. The mechanical properties of the NBR nanocomposites, such as the tensile strength, elongation at break, modulus at different elongation and tear strength relative to the pure NBR are

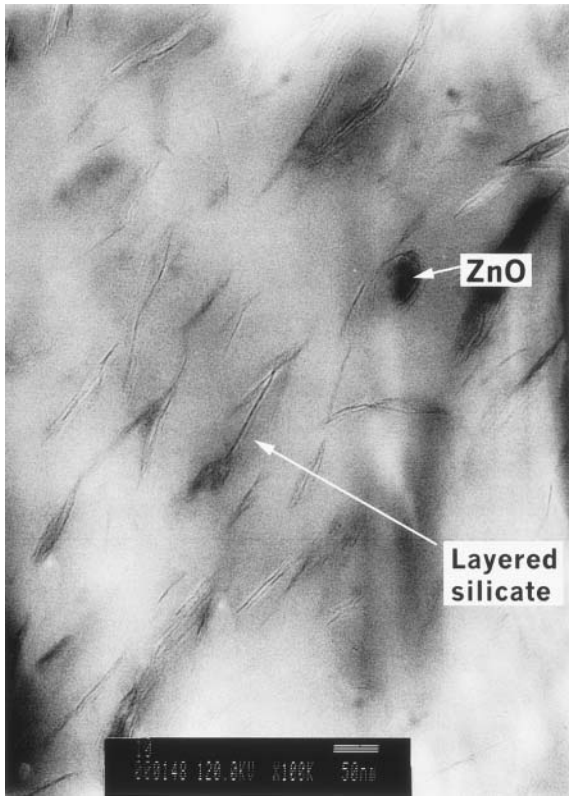

Fig. 2. TEM image taken on the NBR nanocomposite containing 7.5-phr organosilicates.

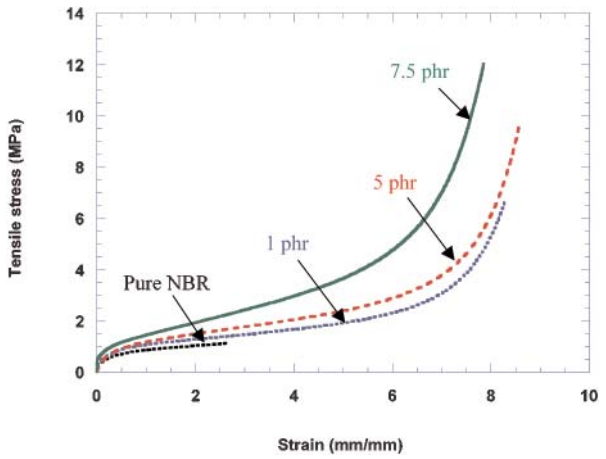

Fig. 3. Typical tensile stress/strain curves of the NBR nanocomposites with various organosilicate contents. [Color figure can be viewed in the online issue, which is available at www.interscience.wiley.com.]

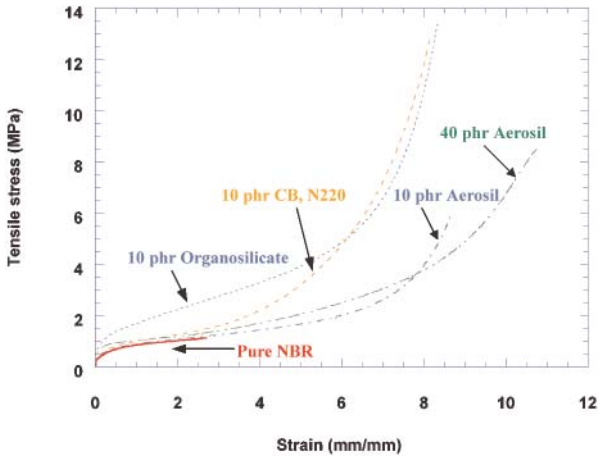

Fig. 4. Typical tensile stress/strain curves demonstrate the reinforcing effect in NBR/organosilicate nanocomposites. [Color figure can be viewed in the online issue, which is available at www.interscience.wiley.com.]

enhanced because of the presence of intercalated/exfoliated layered silicates. A more than sixfold increase in tensile strength, twofold increase in M500, 39% enhancement in elongation at break, and 267.8% enhancement in tear strength are obtained with the addition of 10 phr of the exfoliated organosilicate. These gains in strength and stiffness without loss in elongation in these nanocomposites are quite different from the behavior of conventional composites. The reinforcing effect is presumed to occur because of intercalated/exfoliated organosilicate layers that are covered by highly crosslinked rubber molecular chains with strong interfacial interactions in between (3, 9, 21).

Figure 4 shows the tensile properties of NBR containing organosilicate, high strengthening super abrasion furnace carbon black (CB, N220) and silica (Aerosil). The reinforcing effect on NBR by organosilicate appears more pronounced. Particularly, the reinforcing efficiency in the tensile modulus is higher than that of NBR/CB compound under 600% strain. For instance, only 3 to 5 parts of organosilicate are enough to obtain a comparable tensile strength to that of NBR containing 40 parts of Aerosil. In the conventional carbon black, the reinforcing effect was interpreted as bound rubber phenomenon involves physical adsorption, chemisorption, and mechanical interaction (28).

Infrared spectra of the polymer nanocomposites can be used to illustrate the occurrence of chemical reactions or strong interactions between polymer and reinforcers (12, 21, 30, 31). Polymer/layered silicate nanocomposites are difficult to analyze because of the reflective properties of the layered silicate platelets. *Figure 5* shows FTIR spectra, over a frequency range of 950−1600 cm^{-1}, of organosilicate as received, cured NBR/organosilicate and pure NBR compounds, Absorption peaks are observed at 1010, 1041, 1129 (C=S not linked to N), 1200 (C=S not linked to N), and 1242 (C=S linked to N) cm^{-1}, which are characteristic of cured pure NBR compound. The peaks at 1010 and 1041 cm^{-1}, attributed to sulfoxide stretching vibrations, shift to 1040 and 1077 cm^{-1} in the NBR/organosilicate nanocomposite, owing to the interference effect of Si-O stretching vibrations in layered silicates. The peaks at 1129, 1200, and 1242 cm^{-1}, attributed to the accelerator reaction products (cyclohexyl benzthiazyl sulfonamide (CBS) and dibenzthiazyl disulphide (DM)) and sulfur, disappear in the NBR nanocomposite, whereas a medium and broad absorption band at approximately 1217 cm^{-1} appears. This indicates that a strong interaction between layered silicates and the curative reaction products exists and results in a new absorption peak in the NBR nanocomposite. The interesting outcome is the appearance of a C-SO_2-N

Table 3. Mechanical Properties of NBR Compounds.

Organosilicate Content (phr)	Hardness	Tensile Strength (MPa)	Elongation at Break (%)	M100 (MPa)	M300 (MPa)	M500 (MPa)	Tear Strength (kg/cm)
0	46	2.1 ± 0.2	600 ± 54	0.89 ± 0.01	1.24 ± 0.03	1.73 ± 0.07	8.7 ± 0.1
1	49	6.2 ± 1.6	521 ± 46	1.09 ± 0.01	1.51 ± 0.03	2.02 ± 0.07	11.6 ± 1.0
3	51	7.9 ± 0.9	816 ± 31	1.10 ± 0.02	1.64 ± 0.04	2.25 ± 0.07	14.2 ± 0.6
5	53	9.5 ± 1.6	826 ± 27	1.21 ± 0.02	1.81 ± 0.03	2.45 ± 0.07	15.3 ± 0.6
7.5	55	12.0 ± 2.2	784 ± 52	1.43 ± 0.03	2.42 ± 0.10	3.59 ± 0.21	19.8 ± 0.5
10	57	13.4 ± 1.8	833 ± 21	1.70 ± 0.03	2.70 ± 0.09	3.85 ± 0.13	23.3 ± 0.1

M100: engineering modulus at 100% elongation.
M300: engineering modulus at 300% elongation.
M500: engineering modulus at 500% elongation.

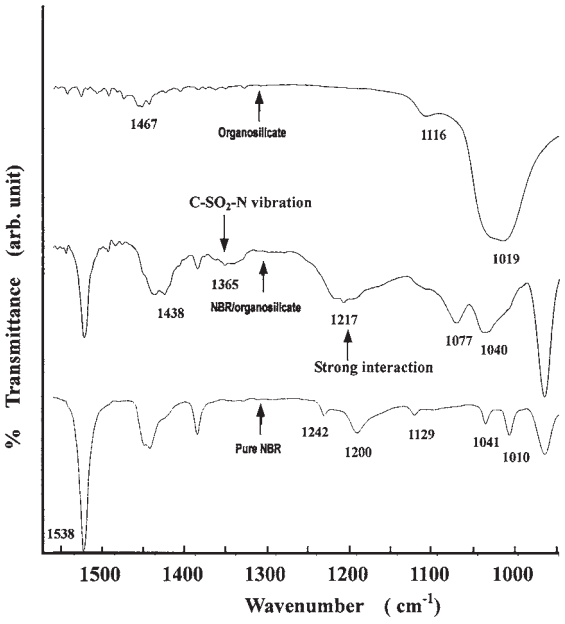

Fig. 5. FTIR spectra of organosilicate, NBR nanocomposite (10 wt% organosilicate) and pure NBR.

bond peak around 1365 cm^{-1} in the NBR nanocomposite, which is absent in the spectrum of pure NBR and of the layered silicates. This may be the result of the possible reaction of an ammonium salt intercalant and zinc-sulfur-amine complexation between the organosilicate and highly polarized NBR during the vulcanization process. Schematic drawings of the possible reaction mechanism are provided in *Fig. 6*. NBR molecular chains were therefore more easily intercalated into the intergallery space of the organosilicate during this process. Recalling the microstructure discussed above, the NBR molecules intercalated into the organosilicate layers could also be considered an effect of bound rubber. This also indicates a strong interaction exists between the intercalated NBR chains and organosilicate layers (6).

The effect of the incorporation of the organosilicate on the crosslinking density of NBR can be estimated by an application of the Flory-Rehner equation. *Table 4* summarizes the crosslinking density and thermodynamical characteristics of the NBR compounds. The crosslinking density is found to increase with the amount of organosilicates. The crosslinking density for the NBR/organosilicate nanocomposite is significantly higher than that of pure NBR. The results are in agreement with those vulcanization characteristics and the tensile properties, indicating a strong rubber/organosilicate interaction (bound rubber) in the nanocomposites. *Table 4* lists the thermodynamical parameters, ΔG and ΔS, of the NBR nanocomposites. A considerable increase in the free energy is observed in the NBR/organosilicate nanocomposites. These results can be attributed to better compatibility between the organosilicate and NBR rubber. The NBR molecules can penetrate into the galleries more easily, and this results in intercalated/exfoliated structures.

Thermal Properties

The thermal properties of NBR nanocomposites were analyzed by TGA and DMA. *Table 5* summarizes the degradation temperatures (Td_5, Td_{50}), storage moduli (E'), glass transition temperatures (T_g), and tanδ values. The degradation temperature at 5% and 50% weight loss were both obtained in this study. The Td_5 decreases with an increasing amount of organosilicate. This is because the alkyl chain-type organo-modifier, such as hydrogenated tallow, begins to decompose above 200°C (32), whereas the resistance of nitrile butadiene rubber molecules to thermal decomposition was improved by the presence of intercalated/exfoliated organosilicate at temperatures higher than 450°C. For instance, the decomposition temperature for a ten-parts' loading of organosilicate on NBR nanocomposite (493°C) was 25°C higher than that of pure NBR (468°C).

The onset storage modulus E', given in *Table 5*, increases as the amount of organosilicate increases. Specifically, the nanocomposites containing 10-phr organosilicate have the highest storage moduli, which are 57% higher than that of pure NBR. These results can be attributed to the larger active surface area and stronger NBR/organosilicate interactions, which is in harmony with the mechanical results. The glass transition temperature was obtained from the peak temperature of tanδ as depicted in *Table 5*. Decreases in T_g and tanδ also occur as the organosilicate content increases. Similar results were reported and rationalized for ammonium salt intercalated in silicate layers that may act as a plasticizer or lubricant (16, 32).

Barrier Properties

Figure 7 highlights the barrier improvement of NBR-based nanocomposites against water and methanol vapor. The relative vapor permeability of the NBR rubber is reduced markedly by 85% (from 100% to 15%) for water and by 42% (from 100% to 58%) for methanol, whereas the permeability values for water and methanol are 967 and 5111 g/m^2/day, respectively. This indicates the intercalated/exfoliated NBR/silicate nanocomposites improve the vapor barrier properties dramatically. It is noteworthy that the methanol permeability results agree with the crosslinking density results discussed above. Therefore, the permeability is controlled by the microstructure of the nanocomposite and the interaction between NBR and organosilicates.

The enhancement of mechanical properties of NBR nanocomposites formed by the solution-blending process presented in this study is more dramatic than that found in NBR nanocomposites obtained by the melt-mixing or latex-blending process, as reported in the literature (18–20). For example, a sixfold increase in the tensile strength without a loss in the ultimate elongation by the solution method has been achieved, as opposed to a threefold to fourfold increase of tensile strength, and a reduction in the elongation, achieved by the conventional melt-mixing process. Permeability test results show the same trends. This can be attributed to two factors. The first is that the interlayer distance of

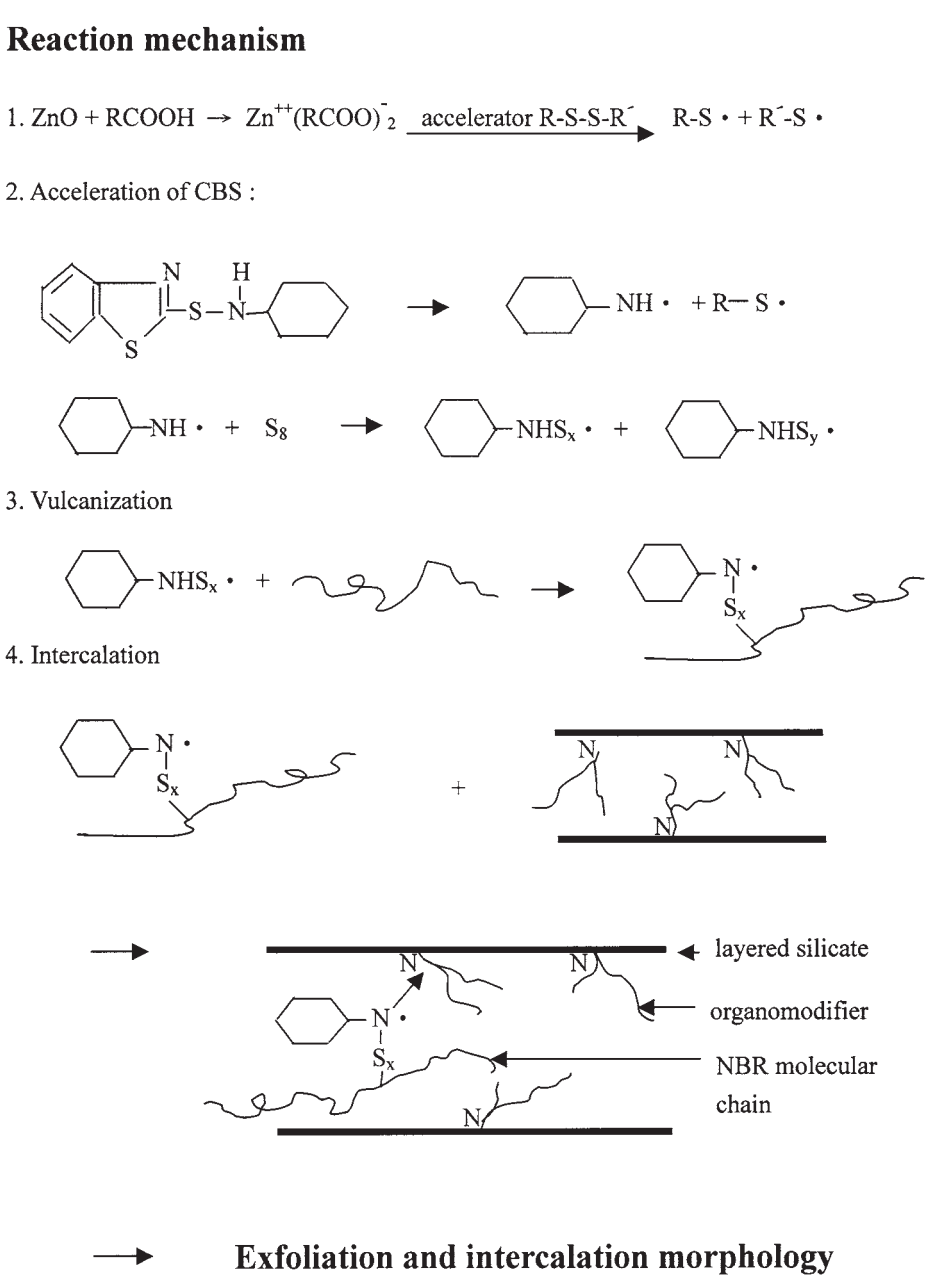

Fig. 6. Possible reaction mechanism of ammonium salt intercalant and zinc-sulfur-amine complexation between organosilicate and highly polarized NBR.

Table 4. Crosslinking Density and Thermodynamical Characteristics of NBR Compounds.

Organosilicate Content (phr)	Volume Volume Fraction	Crosslink Density (mol/cm^3)	ΔG (Jmol^{-1})	ΔS (Jmol^{-1} K^{-1})
0	0.2518	1.995E-04	−26.96	8.899E-02
1	0.2485	1.927E-04	−25.99	8.579E-02
3	0.2547	2.055E-04	−27.83	9.186E-02
5	0.2532	2.024E-04	−27.38	9.035E-02
7.5	0.2687	2.366E-04	−32.32	1.067E-01
10	0.2759	2.538E-04	−34.81	1.149E-01

Table 5. Thermal Properties of NBR Compounds.

Organosilicate Content (phr)	Td_5 (°C)	Td_{50} (°C)	E′ (× 10^9 Pa)	T_g (°C)	Tanδ (= E″/E′)
0	403	468	1.98	−28	1.84
1	371	471	1.13	−25	1.73
3	355	479	1.88	−31	1.78
5	344	477	2.06	−28	1.60
7.5	340	487	2.33	−32	1.55
10	337	493	3.11	−31	1.34

Td_5 (°C): degradation temperature at 5% weight loss.
Td_{50} (°C): degradation temperature at 50% weight loss.

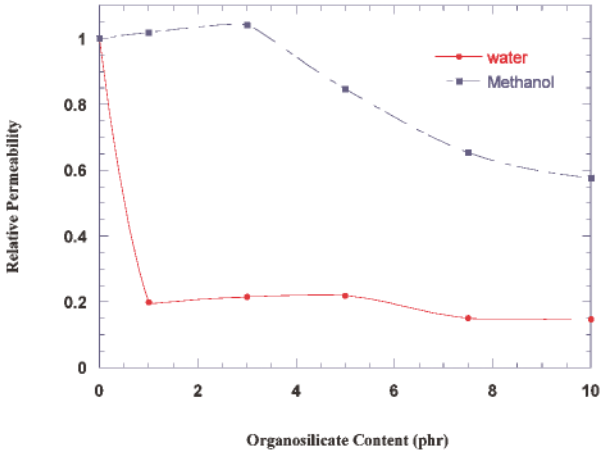

Fig. 7. Relative vapor permeability of NBR nanocomposites containing various amounts of organosilicate. Note: The reference values for water and methanol are 967 and 5111 g/m^2/day, respectively. [Color figure can be viewed in the online issue, which is available at www.interscience.wiley.com.]

layered silicate was expanded more by the solvation effect of MEK than by the melt-mixing method. The agglomerated silicate particles are reduced significantly by shearing forces in the blending stage, which also lead to better dispersion and miscibility of organosilicate in NBR matrix. Finally, the large and coiled nitrile butadiene rubber molecular chains are also swollen and stretched in the good solvent, which is advantageous for intercalation during the blending process.

CONCLUSIONS

NBR/organosilicate nanocomposites with exfoliated and intercalated structures were successfully prepared by the solution-blending method. The hardness, tensile properties and tear strength of these nanocomposites increase substantially with the amount of incorporated organosilicates by containing a few weight-percent of layered silicates, as compared to pure NBR. This reinforcing effect can be attributed to strong interactions between the intercalated NBR molecular chains and organosilicate layers. Additionally, these nanocomposites exhibit higher thermal stabilities and dynamic storage moduli than those of pure NBR. The relative vapor permeability of nanocomposites containing ten parts of layered silicates is reduced by 85% and 42% for water and for methanol, respectively, as compared to pure NBR.

ACKNOWLEDGMENTS

The authors appreciate the financial support provided by the Ministry of Economic Affairs through Project 92FCA12V and the National Science Council through Project NSC91-2120-M-009-001. C. M. Wu also thanks Prof. J. Karger-Kocsis (University of Kaiserslautern, Germany) for a helpful discussion.

REFERENCES

1. A. Usuki, M. Kawasum, Y. Kojima, Y. Fukushima, A. Okada, T. Kurauchi, and O. Kamigaito, *J. Mater. Res.*, **8**, 1179 (1993).
2. M. Kawasumi, N. Hasegawa, M. Kato, A. Usuki, and A. Okada, *Macromolecules*, **30**, 6333 (1997).
3. T. K. Chen, Y. I. Tien, and K. H. Wei, *Polymer*, **41**, 1345 (2000).
4. H. L. Tyan, C. M. Leu, and K. H. Wei, *Chem. Mater.*, **13**, 222 (2001).
5. P. C. LeBaron, Z. Wang, and T. J. Pinnavaia, *Appl. Clay Sci.*, **15**, 11 (1999).
6. Y. T. Vu, J. E. Mark, L. H. Pham, and M. Engelhardt, *J. Appl. Polym. Sci.*, **82**, 1391 (2001).
7. G. Unnikrishnan and S. Thomas, *J. Polym. Sci. Part B*, **35**, 725 (1997).
8. K. S. Kwan, D. A. Harrington, P. A. Moore, J. R. Hahn, J. V. Degroot, and G. T. Burns, *Rubber Chem. Technol.*, **71**, 630 (2001).
9. A. Mousa and J. Karger-Kocsis, *Macromol. Mater. Eng.*, **286**, 260 (2001).
10. Z. Wang and T. J. Pinnavaia, *Chem. Mater.*, **10**, 3769 (1998).
11. J. Karger-Kocsis and C. M. Wu, *Polym. Eng. Sci.*, **44**, 1083 (2004).
12. S. Joly, G. Garnaud, R. Ollitrault, L. Bokobza, and J. E. Mark, *Chem. Mater.*, **14**, 4202 (2002).
13. M. López-Manchado, B. Herrero, and M. Arroyo, *Polym. Int.*, **52**, 1070 (2003).
14. M. Arroyo, M. López-Manchado, and B. Herrero, *Polymer*, **44**, 2447 (2003).
15. S. Varghese, J. Karger-Kocsis, and K. G. Gatos, *Polymer*, **44**, 3977 (2003).
16. F. Schön, R. Thomann, and W. Gronski, *Macromol. Symp.*, **189**, 105 (2002).
17. A. Usuki, A. Tukigase, and M. Kato, *Polymer*, **43**, 2185 (2002).
18. W. G. Hwang, K. H. Wei, and C. M. Wu, *Polymer*, **45**, 5729 (2004).
19. J. T. Kim, T. S. Oh, and D. H. Lee, *Polym. Int.*, **52**, 1203 (2003).
20. C. W. Nah, H. J. Ryu, W. D. Kim, and S. S. Choi, *Polym. for Adv. Technol.*, **13**, 649 (2002).
21. Y. I. Tien and K. H. Wei, *Macromolecules*, **34**, 9045 (2001).
22. T. K. Chen, Y. I. Tien, and K. H. Wei, *J. Polym. Sci., Part A: Polym. Chem.*, **37**, 2225 (1999).
23. Y. I. Tien and K. H. Wei, *J. Polym. Res.*, **7**, 245 (2000).
24. S. D. Burnside and E. P. Giannelis, *Chem. Mater.*, **7**, 1597 (1995).
25. P. C. LeBaron and T. J. Pinnavaia, *Chem. Mater.*, **13**, 3760 (2001).
26. Y. I. Tien and K. H. Wei, *Polymer*, **42**, 3213 (2001).
27. L. H. Sperling, *Introduction to Physical Polymer Science*, 2nd ed., Chap. 9, p. 382, John Wiley & Sons, New York (1993).
28. M. Morton, ed., *Rubber Technology*, Van Nostrand Reinhold, New York (1985).
29. C. I. Park, O. O. Park, J. G. Lim, and H. J. Kim, *Polymer*, **42**, 7465 (2001).
30. E. Passaglia, W. Bertuccelli, and F. Ciardelli, *Macromol. Symp.*, **176**, 299 (2001).
31. M. Pramanik, S. K. Srivastava, B. K. Samantaray, and A. K. Bhowmick, *J. Polym. Sci. Part B: Polym. Phys.*, **40**, 2065 (2002).
32. Y. S. Choi, M. H. Choi, K. H. Wang, S. O. Kim, Y. K. Kim, and I. J. Chung, *Macromolecules*, **34**, 8978 (2001).